Long-term patterns of hydrocarbon biodegradation and bacterial community composition in epipelagic and mesopelagic zones of an Arctic fjord.

Ioannis D. Kampouris[*1,2], Friederike Gründger[1,2], Jan H. Christensen[3], Charles W. Greer[4], Kasper Urup Kjeldsen[5], Wieter Boone[7], Lorenz Meire[8,9], Søren Rysgaard[1,2,10], Leendert Vergeynst[*1,6]

1. Arctic Research Centre, Department of Biology, Aarhus University, Aarhus, Denmark
2. Section for Aquatic Biology, Department of Biology, Aarhus University, Aarhus, Denmark
3. Department of Plant and Environmental Sciences, Faculty of Science, University of Copenhagen, Copenhagen, Denmark
4. National Research Council Canada, Energy, Mining and Environment Research Centre, Montreal, Canada
5. Section for Microbiology, Department of Biology, Aarhus University, Aarhus, Denmark
6. Centre for Water Technology (WATEC), Department of Biological and Chemical Engineering, Aarhus University, Aarhus, Denmark
7. Flanders Marine Institute, 8400 Oostende, Belgium
8. Department of Estuarine and Delta Systems, Royal Netherlands Institute of Sea Research, Yerseke 4401 NT, The Netherlands
9. Greenland Climate Research Centre, Greenland Institute of Natural Resources, Nuuk 3900, Greenland
10. Centre for Earth Observation Science, University of Manitoba, Winnipeg, MB, Canada

*Corresponding authors:

Ioannis D. Kampouris,
Arctic Research Centre,
Department of Biology,
Aarhus University, 8000,
Aarhus, Ny Munkegade 114,
Denmark,
E-mail: ioannis.kampouris@bce.au.dk

Leendert Vergeynst,
Centre for Water Technology (WATEC),
Department of Biological and Chemical Engineering,
Aarhus University, 8000,
Aarhus, Universitetsbyen 36,
Denmark,
E-mail: leendert.vergeynst@bce.au.dk

Keywords: Oil biodegradation; Arctic; Microbiome; Oil-degrading bacteria

Abstract

Oil spill attenuation in Arctic marine environments depends on oil-degrading bacteria. However, the seasonally harsh conditions in the Arctic such as nutrient limitations and sub-zero temperatures limit the activity even for bacteria capable of hydrocarbon metabolism at low temperatures. Here, we investigated whether the variance between epipelagic (seasonal temperature and inorganic nutrient variations) and mesopelagic zone (stable environmental conditions) could limit the growth of oil-degrading bacteria leading to lower oil biodegradation rates in the epipelagic than in the mesopelagic zone. Therefore, we deployed absorbents coated with three oil types in a SW-Greenland fjord system at 10-20 m (epipelagic) and 615-650 m (mesopelagic) water depth for one year. During this period we monitored the development and succession of the bacterial biofilms colonizing the oil films by 16S rRNA gene amplicon quantification and sequencing, and the progression of oil biodegradation by gas chromatography – mass spectrometry oil fingerprinting analysis. The removal of hydrocarbons was significantly different, with several polycyclic aromatic hydrocarbons showing longer half-life in the epipelagic than in the mesopelagic zone. Bacterial community composition and density (16S rRNA genes/ cm^2) significantly differed between the two zones, with total bacteria reaching to log-fold higher densities (16S rRNA genes/cm^2) in the mesopelagic than epipelagic oil-coated absorbents. Consequently, the environmental conditions in the epipelagic zone limited oil biodegradation performance by limiting bacterial growth.

1. Introduction

Climate change will prolong ice-free regions in the Arctic, intensifying transarctic shipping and the risks of major oil spill accidents (Miller and Ruiz, 2014). Oil spilled in the open sea disperses into small oil droplets, which get entrained in the water column followed by dissolution, photo-oxidation and biodegradation. The relative importance of these processes depends strongly on the chemical properties of the oil hydrocarbons including alkanes, isoprenoids; and monoaromatic and polycyclic aromatic hydrocarbons (Tissot and Welte, 1978; Head et al., 2006).

Following dispersion, dissolution and evaporation mainly remove the low molecular weight hydrocarbons including short-chain alkanes and aromatic compounds with typically less than three aromatic rings and a low degree of alkylation (Vergeynst et al., 2018a; Murphy et al., 2021). The dissolved aromatic compounds with one to three rings have a biological half-life of 25 to 105 days that generally increases with the degree of aromaticity and alkylation in Arctic seawater at 0°C (Gomes et al., 2021). For the removal of the less soluble compounds, aliphatic compounds can degrade with half-life times of as short as 7 days when sufficient nutrients are available (Vergeynst et al., 2019a). However, the high molecular weight and least water-soluble polycyclic aromatic compounds (typically alkylated and with more than three aromatic rings) degrade with extremely slow rate (half-life of at least 60 days) and depend on photo-oxidation and biofilm-mediated biodegradation of dispersed oil droplets (Kimes et al., 2014; Vergeynst et al., 2018a; Scheibye et al. 2017). Photo-oxidation contributes to the removal of polycyclic aromatic hydrocarbons by oxidizing the aromatic rings, which increases their water solubility and emulsification (Shankar et al., 2015; Li and Garrett, 1998; Maki et al., 2001; Péquin et al., 2022).

Psychrophilic oil-degrading bacteria mediate oil biodegradation even at subzero temperatures (Margesin and Schinner, 1999; McFarlin et al., 2014, Vergeynst et al., 2019b; Murphy et al., 2021). Due to the high viscosity and low solubility of petroleum, marine bacteria form a biofilm layer at the water/oil

interphase that enables their access to hydrophobic hydrocarbons (Omarova et al., 2019). Hydrocarbon-degrading bacteria generally occur in low abundance in seawater, but bloom upon oil spills (Atlas and Hazen, 2011). Psychrophilic hydrocarbon-degraders in marine Arctic waters, particularly *Oleispira* spp., are known to mediate alkane degradation and typically bloom in the early stage of oil-exposure (Ribicic et al., 2018; Vergeynst et al., 2018a; Vergeynst et al., 2019a; Vergeynst et al., 2019b; Nikolova et al. 2022). *Oleispira* spp. are frequently succeeded by polycyclic-aromatic-hydrocarbon degrading bacteria, such as *Cycloclasticus* spp. and C1-B045, which appear only at the later stages of biodegradation (Brakstad et al., 2018; Peng et al. 2020; Nikolova et al. 2022). Usually the various zones (epipelagic, mesopelagic and bathypelagic) have distinct differences in environmental conditions, such as nutrient content and temperature. Most of the previous studies have focused on the oil biodegradation patterns in low temperatures by performing lab experiments or *in situ* experiments at a specific depth, neglecting the effect of environmental conditions in different zones on oil biodegradation patterns.

One of the main differences between the zones is the availability of inorganic nutrients, and especially the phosphorus and nitrogen content (Guo et al., 2018). The combination of high carbon load with low content of nitrogen and phosphorus limits oil biodegradation performance in oil spills (Shiller and Joung, 2012; Nõlvak et al., 2021). These nutrient limitations are particularly pronounced in Arctic marine waters, which have low nitrogen and phosphorus content (Sala et al., 2010). Nitrogen and phosphorus become depleted at the epipelagic zone (0-200 m) during the summer season (Frette et al. 2010), due to blooms of phototrophic plankton and water column stratification (Reigstad et al., 2002; Tamelander et al., 2009; Tremblay et al., 2012; Randelhoff et al., 2020). In contrast, their availability increase during winter as the water column is mixed and low-light intensities and ice cover limit phototrophic growth. Meanwhile, nutrient concentrations remain stable deeper in the water column (mesopelagic zone, 200-1000 m) (Reigstad et al., 2002; Tamelander et al., 2009; Tremblay et al., 2012; Randelhoff et al., 2020). In addition, the temperature of seawater in surface drops below 0^{o} C during the

winter, whereas it remains stable over the year in the mesopelagic zone (Mortensen et el., 2011). Temperatures below 0° C strongly reduce microbial activity of oil blooms (Lofthus et al., 2021), despite the higher concentration of inorganic nutrients in the winter than in the summer months. The combination of low inorganic nutrients in the summer and lower temperatures during winter might restrict the oil biodegradation in the epipelagic zone, however there is a lack of field observations on whether these environmental features could affect the potential for oil biodegradation differently in the epipelagic and mesopelagic zone in Greenlandic waters. Consequently, we here tested the hypothesis that the nutrient and temperature variations across seasons in the epipelagic zone will limit the growth of oil degrading bacteria leading to lower oil biodegradation rates, when compared to the mesopelagic zone.

To test this hypothesis, we performed an *in situ* experiment in a Greenlandic fjord for over one year, which is one the longest biodegradation *in situ* experiment that has been performed up to now. We coated adsorbents (hydrophobic fluorocarbon-based mesh nets) with thin oil layers to simulate dispersed oil droplets in the water column (Brakstad et al., 2006; Vergeynst et al., 2019a; Vergeynst et al., 2019b) and investigated the bacterial biofilms colonizing and degrading the oil. The adsorbents were deployed for up to one year in the epipelagic and mesopelagic zone and sampled after 8, 37, 100 and 379 days. Samples were analyzed by gas chromatography - mass spectrometry (GC-MS) to quantify 13 selected oil hydrocarbons, and PCR amplicon sequencing and quantification of the 16S rRNA gene for evaluating the bacterial composition and biomass densities of the observed hydrocarbon-degrading biofilms.

2. Materials and Methods

2.1 Field experiment with *in situ* oil-coated adsorbents

For the *in situ* experiments, we deployed moorings (Fig. S1) with adsorbents (hydrophobic fluorocarbon-based poly(ethylene-co-tetrafluoroethane) mesh nets, Sefar Inc., production reference 09-250/39, dimensions 90 × 45 × 0.29 mm) coated with thin layers of oil as described in previous studies (Vergeynst et al., 2019a; Vergeynst et al., 2019b). Three oil types were used: a) a distillate oil (marine gas oil, MGO, Kuwait Petroleum, Denmark), b) a light crude oil (troll blend crude oil, TBC-crude, ExxonMobil, Norway), and c) a highly in-source biodegraded light crude oil (HBC-crude, source undisclosed). The adsorbents were coated with oil 5-15 min before deployment in the water column. The adsorbents were deployed in the epipelagic zone in Kobbefjord (N64°08.684 W51°35.939) and in the mesopelagic zone (N64°37.008 W50°56.927) in the adjacent Godthåbsfjorden/Nuup Kangerlua (SW Greenland) in May 2018 (Fig. S2). The epipelagic adsorbents were deployed approximately at 8 m above the sea floor and approximately 4-20 m (due to tidal variations) below sea surface, where they were exposed to seasonal nutrient and temperature variations (Middelboe et al., 2012; Meire et al., 2016; Gluchowska et al., 2017). The photic zone extends from 20 - 57 m depending on seasonality (Sejr et al., 2014). Mesopelagic zone adsorbents were deployed at 35 m above the sea floor (about 615-650 m depth due to tidal variations) in Godthåbsfjorden, where stable nutrient and temperature conditions occur throughout the year (Middelboe et al., 2012; Meire et al., 2016). The experiment lasted for 379 days (30/05/2018 - 03/06/2019).

We deployed four moorings at both sites, which were recovered after 8, 37, 100, and 379 days of exposure. The absorbents were shielded from light to avoid photo-oxidation. Oil- and non-coated adsorbents were mounted on the same moorings at about 20 cm distance. From each mooring, four oil-coated absorbents of each type of oil (distillate, HBC-crude and TBC-crude) and four non-coated (control) absorbents were used. Two adsorbents for chemical analysis were transferred to glass vials and the

residual oil on the adsorbents extracted in 7 ml SupraSolv dichloromethane (Merck) and stored in the dark at 4°C. The two other adsorbents for DNA extraction were transferred to 50 ml Falcon centrifuge tubes filled to capacity with RNA*later* (Thermo Fisher Scientific) and stored at -20°C. Duplicate seawater samples (960 mL) collected at the same depths (20 and 650 m) at the moorings for DNA extraction were filtered on Sterivex filters and stored with RNA*later*. Temperature, salinity and the concentrations of total dissolved phosphate, nitrate, nitrite and ammonia in the seawater were measured as described by Meire et al. (2016).

2.2 Gas chromatography - mass spectrometry

GC-MS analysis was performed as described previously (Gallotta and Christensen, 2012). Samples were purified and dried over Na_2SO_4. In the analytical sequence, a solvent blank (dichloromethane), distillate, TBC-crude and HBC-crude oil standards and a mixture sample of the three oils as quality control were analyzed after every seventh sample. Chromatograms were aligned using Matlab, as described previously (Tomasi et al., 2004; Tomasi et al., 2011, Skov et al., 2006) and peak areas were determined by automatic integration with the lower convex hull as baseline using programming language R (v. 4.1.1, R Core Team, 2019). The biomarkers 17α(H),21β(H)-hopane and a C_{24} tricyclic diterpane were used as internal standard to quantify depletion of oil compounds from adsorbents coated with the crude oils (TBC- and HBC-crude) and the distillate oil, respectively (Table S2). For the analysis of biodegradation, we selected 13 poorly water-soluble groups of hydrocarbons exhibiting less than 20 % dissolution after 60 days in seawater (Fig. 1 & Fig. S3), as described in Section S1 (Supplementary Information, SI). The selected hydrocarbons include aliphatic compounds (C_{14-35} *n*-alkanes, isoprenoids and C_2-decalins) and polycyclic aromatic hydrocarbons (C_{3-4}-phenanthrenes, C_{3-4}-dibenzothiophenes, C_{1-2}-pyrenes, C_{0-2}-chrysenes). On the other hand, mono-aromatics and non-alkylated polycyclic aromatic hydrocarbons were excluded due to higher than 20 % removal by dissolution (Fig.

S3). Since dissolution was negligible (<20% removal) for the selected hydrocarbons and photo-oxidation was excluded by the experimental setup, the hydrocarbon removal in the field experiment can be mainly explained by biodegradation.

2.3. DNA extraction, qPCR, and high-throughput amplicon sequencing of the 16S rRNA gene

DNA extractions were performed based on the protocol by Lever et al. (2015) with slight modifications: the washing process was repeated two times and sterivex filters, which contained RNA*later* solution, were flushed with 10 ml sterile deionized water before DNA extraction. As a proxy for bacterial density developing as a biofilm on the adsorbents, we quantified the amount of bacterial 16S rRNA gene (genes/cm^2) by quantitative real-time PCR (qPCR) as described by Starnawski et al. (2017) with the primer pair Bac908F/Bac1075R and SYBR Green-based technology. For PCR amplicon sequencing, fragments covering the V3-V4 region of the 16S rRNA gene were amplified with (KAPA Biosystems) using the primer pair Bac341F/Bac805R (Herlemann et al., 2011) in a first round of PCR. In a second PCR, the PCR products were supplied with Illumina adaptor overhang sequences. PCR purification, indexing with the Nextera XT Index Kit (Illumina), library quantification, pooling, and sequencing were performed following Illumina's protocol as described previously (Vergeynst et al., 2018b). Pooled libraries were sequenced on an Illumina MiSeq system using a 600 cycle MiSeq v3 Reagent Kit (Illumina), which produces 300-bp long paired-end reads.

2.4 Bioinformatics, data analysis, and statistics

All data handling and statistical analyses were performed with the programming language R (v. 4.1.1, R Core Team, 2019). The “tidyverse” set of packages (v1.3.1, Wickham et al., 2019) was used for

handling the data and performing data transformations. The package "ggplot2" (v3.3.5.9, Wickham, 2016) was used for graphical representations.

2.4.1 Handling of chemical data and statistics

To compare the composition of poorly water-soluble hydrocarbons for the two zones (epipelagic versus mesopelagic zone) and exposure time, we performed principal component analysis (PCA) and PERMANOVA using the package "vegan" (v2.5.7, Oksanen et al., 2020). The permutation-based beta-dispersion test (function "betadisper", package "vegan") was used to evaluate whether the significance of the observed PERMANOVA *p*-values was influenced by the heterogeneity of the variance between groups. All tests had *p*-values higher than 0.05, indicating that heterogeneity of variance did not influence the observed differences in PERMANOVA tests. The degradation rates and half-life time of compounds were calculated based on a first-order growth and degradation model published in a previous study (Gomes et al., 2019), with minor modifications: the unitless fraction (X_0/C_0) was set to 0.1 for alkanes and 0.05 for the other compounds to avoid overfitting. Linear mixed-effect models were used for estimating the effect of zone on the biodegradation. Available nitrogen concentration (total-nitrogen= nitrate + nitrite + ammonia) was calculated for estimating whether nitrogen could be the limiting factor for biodegradation.

2.4.2 Processing of the raw reads

Paired-end reads were processed using the DADA2 pipeline (Callahan et al. 2016). The obtained amplicon sequence variants (ASVs) were taxonomically classified down to the lowest possible taxonomic level based on the SILVA SSU Reference Taxonomy v132 (Quast et al., 2013; Yilmaz et al., 2014), using a Naive Bayesian Classifier (Wang et al., 2007). Singletons and sequences identified as

chloroplast or mitochondria were removed. Rarefaction curves showed that the sequencing depth sufficiently covered the diversity of each sample (Fig. S4). A phylogenetic tree of ASVs was generated with fastree2 (Price et al., 2010) for estimating the ASV phylogenetic distance. PCR amplicon sequence data has been deposited at the Sequence Read Archive (https://www.ncbi.nlm.nih.gov/sra) under the BioProject accession (PRJNA884198).

2.4.3 Amplicon Sequencing data analysis

The β-diversity was calculated using the weighted UniFrac distance (Lozupone et al., 2011). For the analysis of the bacterial community compositions, we divided the adsorbents in accordance to oil-exposure: non-coated and oil-coated adsorbents. To test whether *exposure time*, *oil-exposure* and *zone* significantly affected the β-diversity, we used PERMANOVA tests as described in Section 2.4.1. The multivariate correlation between hydrocarbon removal and the β-diversity was quantified using a Mantel test and Procrustes test ("vegan"). The bacterial biomass developing as a biofilm on the adsorbents was normalized to the total surface of both sides of the adsorbents (81 cm^2) and expressed as bacterial density, expressed as 16S rRNA genes/cm^2. To identify oil-associated ASVs, we calculated the density of each ASV expressed as 16S rRNA genes/cm^2 by multiplying the relative abundance (amplicon sequencing data) with the qPCR-derived total bacterial density (16S rRNA genes/cm^2).

For investigating the effect of oil-exposure and zone on ASV densities and relative abundance, the non-parametric mixed-effect test Aligned-Rank Transform ANOVA (package "ARTool", v. 0.11.1, Kay et al., 2021) with exposure time as random effect was used. ASVs were reported as oil-associated when the effect of oil treatment was significant ($p < 0.05$ following Benjamini-Hochberg correction) and their density was at least 10-fold higher in oil-coated than non-coated adsorbents for at least one of the zones and time points. We also compared the effect of *oil-exposure* and *zone* on the cumulative relative abundance and cumulative densities of oil-associated ASVs using Aligned-Rank Transform ANOVA,

238 which we defined as total sum of the relative abundances or densities of oil-associated ASVs in each
239 sample, respectively.

3. Results

3.1 General performance of the *in situ* experiment

The concentration of bulk oil on the adsorbents, quantified using the conserved biomarkers (17α(H),21β(H)-hopane and a C_{24} tricyclic diterpane) as internals standards, was lower for distillate (0.27-1.4 mg/cm^2) than for the TBC-crude (0.78-4.0 mg/cm^2) and HBC-crude (1.3-3.1 mg/cm^2) oil. These amounts correspond to equivalent oil droplet diameters of 19-98, 55-284 and 92-219 µm for distillate, TBC-crude and HBC-crude oil, respectively (Table S2). The amount of oil generally decreased with time due to physical detachment of oil from the adsorbents, which should not be considered as a biological degradation process. Also, turbulence during the deployment caused some oil dispersion from oil-coated to non-coated adsorbents, because adsorbents with and without oil coating were mounted on the same moorings at about 20 cm distance. The chemical analysis revealed this cross-contamination to be minor with maximal observed oil concentrations on non-coated adsorbents corresponding to 0.5% of the oil concentration on the initial oil-coated adsorbents (Table S3).

During the long-term incubation, biofilm was successfully grown on the adsorbents. This indicated the success of the experimental design to simulate the biofilm colonization on dispersed oil droplets during long-term incubation. The bacterial densities on the oil-coated absorbents increased from 4.8 ± 0.8 to 7.8 ± 0.4 $\log_{10}$ 16S rRNA genes/cm^2 between 8 and 37 days and remained at similarly high values throughout the whole experiment (Fig. S5). The bacterial densities on the non-coated absorbents remained low for the whole experiment in mesopelagic zone (5.2-5.7 $\log_{10}$ 16S rRNA genes/cm^2, Fig. S5), whereas they increased in epipelagic zone between 37 and 100 days and remained similarly high (8 days: 5.5 ± 0.1, 37 days: 5.0 ± 0.3, 100 days: 5.7 ± 0.3, 367 days: 7.1 ± 0.3 $\log_{10}$ 16S rRNA genes/cm^2; Fig. S5).

Mesopelagic seawater samples had higher concentrations of total nitrogen (11.93 - 14.83 µM between 8 and 100 days) as compared to epipelagic seawater samples (0.52 - 3.08 µM between 8 and

100 days, Table S4). Phosphate concentrations in the epipelagic zone had similar trends (Epipelagic Zone: 0.09-0.28 μM between 8-100 days; Mesopelagic Zone: 0.82-0.85 μM between 8 and 100 days, Table S4). Over the year, temperature remained stable in the mesopelagic (+0.7 - +1.9 ^{o}C), while it showed a seasonal variation in the epipelagic zone (-1.1 - +6.7 ^{o}C, Fig. 2A). Since these samplings were performed over the summer (June-September), the results confirm the expected variations in environmental conditions between the zones. Salinity was slightly higher in the mesopelagic (33.5 ± 0.0 PSU) than epipelagic zone (32.3 ± 0.8 PSU) over the year (Fig. 2B), but did not differ between the two zones as highly as the concentration of inorganic nutrients. However, salinity showed a decrease from 33.08 to 28.3 PSU over summer in the epipelagic zone, showing the effect of seasonal variability on the epipelagic zone. In contrast, salinity remained stable in the mesopelagic zone, with values ranging from 33.4 to 33.6 PSU (Fig. 2B), indicating the lower effect of variations of environmental conditions on the mesopelagic zone.

3.2 Hydrocarbon degradation patterns differed between the two zones

Oil biodegradation occurred in both zones, and generally we observed removal rates that decreased and half-life times increased with the structural complexity of hydrocarbons (higher molecular weight, more rings and more alkylation, Fig. 1). The aliphatic hydrocarbons (i.e. $C_{14\text{-}21}$ n-alkanes, $C_{22\text{-}35}$ n-alkanes and isoprenoids) had the shortest half-life times (20 - 66 days, Fig. 1, Table 1). C_2-decalins had two-fold longer half-life times (43 - 128 days, Table 1) than *n*-alkanes and isoprenoids, whereas polycyclic aromatic hydrocarbons had the highest half-life times (ranging from 138 to 450 days). The polycyclic aromatic hydrocarbons with most rings and alkylation, $C_{1\text{-}2}$-chrysenes, had the longest half-life times (268 - 430 days, Fig. 1 & S6, Table 1). After one year, the amount of removal ranged from nearly 100% for the aliphatic compounds to 48 to 98 % for the alkyl-substituted polycyclic aromatic

hydrocarbons (three-four aromatic rings), with the least removal observed for the C_2-chrysenes (48 - 72 %).

Time, *oil-type* and *zone* significantly explained 92, 1.3 and 0.7 % of the total variation in the multivariate space of 13 compounds respectively (PERMANOVA, $p < 0.001$, Fig. 3A, n = 2 - 16, Table 2). The degradation pattern of the poorly water-soluble hydrocarbons increasingly differed between the two zones over time, as shown by the correlation of increasing Euclidean distance with time for the TBC- and HBC-crude oil (Spearman $r >= 0.9$, $p < 0.05$, Fig. 3B). However, no such correlation was observed for distillate oil (Spearman r = 0.4, $p > 0.05$, Fig. 3B), where the maximum difference was observed after 37 days.

The linear mixed effect model (*Removal ~ Zone* + 1|*Time:Oil-Type*) indicated that the removal of polycyclic aromatic hydrocarbons was significantly lower in the epipelagic than the mesopelagic zone for most alkyl-substituted polycyclic aromatic hydrocarbons (C_{3-4}-phenathrenes, C_{3-4}-dibenzothiophenes and C_{1-2}-chrysenes; n = 48, $p < 0.05$) but not for the rest of hydrocarbons (chrysene, C_{1-2}-pyrenes/fluoranthenes, C_2-decalins, isoprenoids, C_{14-21} alkanes, and C_{22-35} alkanes; n = 48, $p > 0.05$). In particular the degradation rates of polycyclic aromatic hydrocarbons were lower in the epipelagic zone with half-life times of 304.7 ± 119.5 and 275.5 ± 106.1 days for TBC-crude and HBC-crude oils, respectively, as compared to their corresponding half-life times of 238.3 ± 89.3 and 238.8 ± 74.1 days in the mesopelagic zone (Fig. 1, Table 1). The difference in polycyclic aromatic hydrocarbon degradation rates between the epipelagic and mesopelagic zones was negligible for the distillate oil ($t_{1/2}$ Epipelagic: 175.8 ± 87.6 days; $t_{1/2}$ Mesopelagic: 175.4 ± 68.2 days). Generally, the distillate oil had 20-300 days shorter half-lives for polycyclic aromatic hydrocarbons when compared to the two crude oils (Table 1)

3.3 Bacterial community composition of epipelagic and mesopelagic biofilms

Time, *zone* and *oil-exposure* significantly explained 26, 9 and 6 %, respectively, of the β-diversity variation in the 16S rRNA gene library-derived bacterial community composition of the biofilms colonizing the oil-coated adsorbents (PERMANOVA, $p < 0.001$, n = 16 - 64, Table 3, Fig. 4). To associate the degradation patterns of the poorly water-soluble hydrocarbons with the bacterial community composition, we correlated the dissimilarities of hydrocarbon composition and β-diversity. The weighted UniFrac distance increased significantly with Euclidean distance of the hydrocarbon composition (Fig. 5). This indicated that samples with a more different hydrocarbon composition also had a more different bacterial community composition and vice versa (Mantel test, $r = 0.67$, $p = 1 \times 10^{-5}$, n = 32, Fig 5A). The same conclusion can be derived from the Procrustes test ($r = 0.79$, $p = 1 \times 10^{-5}$, n = 32, Fig. 5B).

3.4 Dominant and oil-associated taxa

To identify oil-associated ASVs (ASVs influenced by oil-exposure), we compared the bacterial densities of ASVs ($\log_{10}$ 16S rRNA genes/cm^2) between oil-coated and non-coated adsorbents over time (Aligned-Rank Transform ANOVA, *Density ~ Oil-exposure + 1|Time*). Out of the total 4651 ASVs, we detected 272 ASVs that differed significantly in terms of density (16S rRNA genes/cm^2) between the oil-coated and the non-coated adsorbents ($p < 0.05$, n = 16 – 48). From these 272 ASVs, 144 were positively associated with the oil-coated adsorbents (Fig. 6; Table S4), while the remaining 128 ASVs occurred in significantly higher densities in non-coated adsorbents (Fig. 6 shows the oil-associated ASVs with $p < 0.001$).

The oil-associated ASVs accounted for 13.1 - 79.8 % of the bacterial community developing on the oil-coated adsorbents (Fig. S7, S8 & S9). Generally, ASVs from the genus *Oleispira* spp. dominated (7.8 - 49.8 % relative abundance) the oil-associated bacterial community composition after 8 and 37 days, in biofilms growing on absorbents coated with all three oil types as well as on non-coated absorbents, in both the epipelagic and mesopelagic samples (Fig. S9). In contrast, *Arcobacter* spp., C1-B045, *Colwellia*

spp., *Cycloclasticus* spp., *Kordia* spp., *Pseudofulvibacter* spp., *Pseudohongiella* spp. and *Ulvibacter* spp. dominated the oil-associated fraction of ASVs after 100 and 379 days (10.1 - 30.9 % relative abundance for each taxon, Fig. 6 & S7).

Oil-associated ASVs appeared on non-coated adsorbents as well, with a maximal relative abundance of 30 % after 37 days (Fig. S8 & S9). The high relative abundance on non-coated adsorbents was caused by contamination with oil from oil-coated adsorbents (Table S3). Our non-coated adsorbents were indirectly exposed to a fraction of dispersed oil droplets during deployment, and contained less than 1% the oil concentration in the oil-coated adsorbents (Table S3). The dispersed oil droplets sustained the moderate growth of oil-degrading bacteria in non-coated adsorbents at comparable relative abundances with oil-coated adsorbents (Fig. S8 & S9). When compared with the oil-coated adsorbents, the non-coated adsorbents contained far lower mass of oil-associated ASVs (Fig. 7). Indeed, total densities of oil-associated ASVs on non-coated adsorbents were one to three orders of magnitude lower than on oil-coated adsorbents, reflecting their growth dependence on the low amounts of oil on non-coated adsorbents (Fig. 7).

3.5 Bacterial biomass densities differed between epipelagic and mesopelagic zones

Moreover, *oil-exposure* and *zone* significantly affected the density of total bacterial ASVs and the cumulative density of oil-associated ASVs in the biofilms (Aligned-Rank Transform ANOVA, *Density ~ Oil-exposure + Zone + Zone:Oil + 1*|Time, $p < 0.05$, Fig. 7). Specifically, the oil-coated adsorbents were colonized faster by total bacteria (and subsequently by oil-associated ASVs) in the epipelagic zone than in the mesopelagic zone, since they had tenfold higher densities on day 8, compared to the oil-coated adsorbents in the mesopelagic zone (Fig. 8). On day 37, both epipelagic and mesopelagic oil-coated adsorbents had similar biofilm densities of oil-associated ASVs (Epipelagic zone: 7.3 ± 0.4, Mesopelagic zone: 8.1 ± 0.4 $\log_{10}$ 16S rRNA genes/cm^2). This trend was reversed on day 100, where the density of oil-associated ASVs peaked in the mesopelagic zone (8.1 ± 0.4 $\log_{10}$ 16S rRNA genes/cm^2, n

= 6) and decreased in the epipelagic zone (oil-coated: 7.1 ± 0.4 $\log_{10}$ 16S rRNA genes/cm^2, n = 6, Fig. 7). The densities reached to similar levels after 379 days (Epipelagic zone: 6.4 ± 0.5, Mesopelagic zone: 6.5 ± 0.8 $\log_{10}$ 16S rRNA genes/cm^2). The biofilm densities of total bacteria and oil-associated ASVs on non-coated adsorbents increased as function of time by one to three orders of magnitude during the initial 100 days in the epipelagic zone, whereas remained relatively stable in the mesopelagic zone, during the same period (Fig. 7). The higher densities on the epipelagic non-coated absorbents is not justified by the contamination due to dispersed oil droplets, since similar amounts of contamination was observed in the epipelagic and mesopelagic non-coated adsorbents (Table S3).

Out of the 144 detected oil-associated ASVs, the biofilm densities of 22 ASVs differed between the epipelagic and mesopelagic zone (Aligned-Rank Transform ANOVA, *Density ~ Oil-exposure + Zone + Zone:Oil + 1|Time*, $p < 0.05$, Fig. 7). These ASVs showed one to ten $\log_{10}$-fold higher or lower densities between epipelagic and mesopelagic (mostly on days 100 and 379). Some of these ASVs were representing up to 30.6 % of relative abundance in some oil-coated absorbents (ASV35 Genus: *Pseudohongiella*) or up to 5-10% (ASV65 Genus: *Kordia* and ASV249 Genus: *Ulvibacter*), while most ASVs did not exceed 0.5 % of relative abundance (e.g. ASV1006, Genus: *Winogradskyella*) (Fig. S11). The association of ASVs with each of the zones followed a taxonomically conserved pattern for *Alteromonadales* (Fig. S11). Several *Alteromonadales* members had higher densities in the epipelagic zone, despite the higher densities of total bacteria in the mesopelagic than the epipelagic zone (Fig. 8) In contrast, ASVs classified as *Ulvibacter* spp. associated with both epipelagic and mesopelagic zone (Fig. S11). Consequently, only a few bacterial taxa occurring in a single niche (epipelagic or mesopelagic zone) shared phylogenetic similarity.

4. Discussion

Biodegradation patterns might show local variation on vertical and horizontal scales of marine waters due to differences in environmental conditions (Powell et al., 2007; Potts et al., 2018). However, bacteria degrade complex hydrocarbons slowly (e.g. alkyl-substituted polycyclic aromatic hydrocarbons), therefore the evaluation of the effect of different environmental conditions requires long-term in situ observations of hydrocarbon degradation patterns. We performed such a unique long-term experiment that revealed how the hydrocarbon biodegradation patterns and rates differed over time within and between epipelagic and mesopelagic zones of Arctic marine waters. Removal of polycyclic aromatic hydrocarbons had approximately 100 days longer half-life times in the epipelagic than the mesopelagic zone. Moreover, the composition of the bacterial communities in biofilms colonizing oil-coated adsorbents significantly differed between the two zones and total bacterial densities reached up to ten-fold higher biomass densities in the mesopelagic than in the epipelagic zone (Fig. 7). This indicated that the environmental conditions in the epipelagic zone, characterized by lower nutrients during summer and lower temperatures during winter, shaped the bacterial community composition and restricted bacterial growth, which in turn had an effect on the biodegradation patterns of alkyl-substituted polycyclic aromatic hydrocarbons.

Biodegradation performance depends on bacterial community composition (Potts et al., 2018). In our samples, biofilm compositions differed per zone, probably due to the difference in environmental conditions, which in turn seems to have played a key role for the biodegradation performance. This is further supported by the significant correlations between the hydrocarbon composition and β-diversity (weighted UniFrac distance) (Fig. 5). 40 out of the 128 (Table S4) oil-associated ASVs (Fig. 8) showed a niche preference between the two zones, which suggests that certain oil-associated bacteria could possess phenotypic traits beneficial for their survival and growth in each of the two zones. However, these traits did not seem to be highly conserved at the different low taxonomic levels (with the exception

of *Alteromonadales*) (Fig. S11). Since we focused on the taxonomic composition of oil-associated ASVs, we lack further insights in the specific phenotypic traits of the oil-associated ASVs that could relate to oil biodegradation. Techniques such as shotgun metagenomics (Schweitzer et al., 2022; Hauptfeld et al., 2022) would be required to reveal such phenotypic traits.

The two investigated zones were characterized by several environmental features that could have shaped the composition of bacterial communities in the oil biofilms: nutrient concentrations, temperature variations and salinity. We hypothesized that one of the important factors behind the altered biodegradation rates and patterns are the consequences of algae blooms in the photic zone during the summer months. The nutrient uptake due to photosynthetic activity in the photic zone causes depletion of nitrogen and phosphate concentrations in epipelagic seawater, which explains the ten-fold lower concentrations in the epipelagic than the mesopelagic seawater that we observed in the present study. In our study, oil-coated adsorbents after 100 days of exposure had half to one order of magnitude higher densities of oil-associated ASVs in the mesopelagic than in the epipelagic zone (Fig. 7), in agreement with nitrogen and phosphorus being considered as the main rate limiting factors behind slow biodegradation rates in the environment (Ron and Rosenberg, 2014; Singh et al., 2014). The lower maximal growth in the epipelagic zone thus highlights the dependence of oil-degrading bacteria on inorganic nutrients to sustain growth and efficiently degrade hydrocarbons.

Geng et al. (2014) reported half-saturation constants for nitrogen during oil biodegradation in marine environments, based on *in-situ* experiments (*n*-alkanes: 50 μM total nitrogen, aromatics: 35 μM total nitrogen). In our study, seawater in the epipelagic and mesopelagic zone had lower nitrogen levels (0.52 - 15 μM) than the predicted half-saturation constants, indicating a similar effect on biodegradation performance. However, the epipelagic zone had the lowest nitrogen concentrations (2.7 - 4.9 μM, Table S4). Aside the predicted half-saturation constants, the ten-fold lower total nitrogen concentrations in epipelagic than mesopelagic seawater indicate higher nitrogen limitations for the growth of oil-degrading

bacteria in epipelagic than in the mesopelagic zone. Apart from nutrient concentrations, temperature and salinity can also be critical factors that shape bacterial communities, thereby influencing biodegradation performance. Usually, salinity above 100 PSU restricts biodegradation (Horel et al., 2012), but the two zones had salinity around 32.9 - 33.5 PSU, which indicates that the salinity difference between the zones did not contribute to the altered oil biodegradation patterns.

The temperature in the epipelagic zone varied throughout the year: in the epipelagic zone, it varied from +6.7°C during summer to -1.1°C in winter, whereas stable temperatures of 0.7 - 1.9°C prevailed in the mesopelagic zone. Since low temperatures are well known to reduce oil biodegradation rates (Bagi et al., 2013; Xue et al., 2015; Vergeynst et al. 2018), we assume that the low temperature in the epipelagic zone during winter months could have limited the bacterial activity, thereby affecting the bacterial community composition and the hydrocarbon biodegradation rates. However, we did not observe an opposite effect: higher biodegradation rates during summer when temperatures were higher in the epipelagic than mesopelagic zone. We conclude that the combination of temperature and nutrient limitations together contributed to the lower biodegradation rates in the epipelagic, rather a single variable on its own.

Due to the presence of icebergs, it was not possible to install epipelagic moorings with oil-coated adsorbents at the same location as the mesopelagic study site. The epipelagic study site was therefore located in a side arm of the fjord closer the open ocean (Figure S2). There are thus other conditions than the previously mentioned nutrients, salinity and temperature such as melted water from icebergs and sea ice, surface runoff water and seawater exchange with the open ocean for which we could not control. The spatial heterogeneity of the epipelagic zone in such fjord systems is high and biodegradation and microbial patterns at different locations might have been influenced by the local hydrodynamic and biochemical conditions. Nevertheless, the typical high seasonal variability of nutrients and temperature

451 are representative for an open water Arctic epipelagic zone and are parameters that are well known and
452 likely to affect oil biodegradation, as discussed above.

453 The overall degradation patterns of poorly water-soluble hydrocarbons followed a similar
454 sequential pattern for the three types of oil, which were similar to previous studies (Kristensen et al.,
455 2015; Scheibye et al., 2017). Aliphatic compounds were nearly completely (90-95 %) degraded after 100
456 days, whereas the removal of heavy molecular weight polycyclic aromatic hydrocarbons occurred
457 between 100 and 377 days (Fig. 1). It is a typical pattern that bacteria degrade structurally less complex
458 compounds initially ($C_{14\text{-}21}$ n-alkanes, isoprenoids, $C_{22\text{-}35}$ n-alkanes and C_2-decalins), whereas the
459 biodegradation of high molecular weight polycyclic aromatic hydrocarbons required longer time and
460 occurred by increasing number of aromatic rings and degree of alkylation, as observed by several
461 laboratory studies as well (Kristensen et al., 2015; Scheibye et al., 2017). While $C_{14\text{-}21}$ *n*-alkanes degraded
462 at the early stage ($t_{1/2}$: 20-66 days), their degradation rate was similar to our previously observed *n*-alkane
463 rates in the area using the same in situ methods: 22–29 % degradation after 24 days in nutrient-depleted
464 seawater during summer (Vergeynst et al., 2019b). In addition, previous studies showed a faster
465 degradation of polycyclic aromatic hydrocarbons due to photo-oxidation (Vergeynst et al. 2019a;
466 Vergeynst et al., 2019b), but persistence of polycyclic aromatic hydrocarbons during biodegradation
467 (Kristensen et al., 2015; Scheibye et al., 2017). Specifically, the polycyclic aromatic hydrocarbon
468 removal was less than 20% after 71 - 77 days (Kristensen et al., 2015). In the present study, we observed
469 half-life time for the polycyclic aromatic hydrocarbons that ranged from 100 to 438 days (Fig. 1), which
470 supports their slow biodegradation in the Arctic marine environments.

471 Despite the similar patterns in the three oils, minor differences were observed for each oil-type.
472 Most polycyclic aromatic hydrocarbons had the shortest half-life time in the distillate oil, in comparison
473 with the two crude oils (Table 1). This comes in agreement with our previous studies, which indicate that
474 biodegradation occurs faster in distillate oils, when compared to crude oils (Vergeynst et al., 2019a). We

observed in this and previous studies that the lower viscosity of the distillate oil led to thinner oil films corresponding to smaller equivalent oil droplet sizes of 19-98 µm for the distillate oil versus 55-284 µm for the crude oils (Table S2), which enhances the bioavailability of poorly water-soluble hydrocarbons (Vergeynst et al., 2019a). Although we did not compare the biodegradability of thin oil films coated on adsorbents with dispersed oil droplets, comparable observations in laboratory studies, with different oil droplet sizes during dispersion, have shown that bioavailability and degradation rates increase for smaller oil droplets due to the enhanced biofilm growth on the total oil-water area (Brakstad et al., 2015). In addition, the overall effect of the *zone* on the half-life of polycyclic aromatic hydrocarbons was lower in distillate oil than the crude oils. The distillate oil has relatively higher levels of alkanes and lower levels of polycyclic aromatic hydrocarbons than the crude oils, which indicates that the oil composition may also play a role on the *zone* effect on hydrocarbon removal.

5. Conclusion

In the present study, we performed a long-term and *in situ* experiment allowed us to estimate half-lives for a range of hydrocarbon compounds in both the epipelagic and mesopelagic zones. Among these, the important group of polycyclic aromatic hydrocarbons were degraded slower in the epipelagic zone. This could possibly be explained by the lower nitrogen/phosphorus concentrations in combination with higher temperature variations in the epipelagic than the mesopelagic zone. This combination of variances in environmental conditions in the epipelagic zone seemed to reduce the biomass of bacterial biofilms and significantly alter bacterial community composition, thereby limiting the biodegradation performance. However, this effect was stronger for the crude oils and weaker for the herein used distillate oil, potentially related to the chemical composition and oil films of the crude oils. Consequently, our results indicate that variability of environmental conditions between pelagic zones (e.g., nutrient concentrations, temperature) and oil spills (e.g., oil composition and droplet size) must be taken into account when planning attenuation strategies for oil spills in Arctic marine environments.

5. Acknowledgments

Lykke Poulsen, Britta Poulsen and Susanne Nielsen from the Department of Biology, Aarhus University, and Kristoffer G. Poulsen and Jette Petersen from the Department of Plant and Environmental Sciences, University of Copenhagen are gratefully acknowledged for the excellent technical laboratory assistance and chemical analyses, respectively. We thank the Greenland Institute of Natural Resources and Egon Randa Frandsen from the Arctic Research Centre for the field logistics support.

6. Funding

This work is a contribution to the Arctic Science Partnership (asp-net.org) and was supported by the research grant 17454 from Villum Fonden and the Multi-Partner Oil Spill Research Initiative (MPRI) of Fisheries and Oceans Canada.

7. References

1) Atlas R.M., Hazen T.C. (2011). Oil biodegradation and bioremediation: A tale of the two worst spills in U.S. history, Environ. Sci. Technol. 45 6709–6715. https://doi.org/10.1021/es2013227.
2) Bagi A., Pampanin D.M., Brakstad O.G., Kommedal R. (2013). Estimation of hydrocarbon biodegradation rates in marine environments: A critical review of the Q10 approach, Mar. Environ. Res. 89 83–90. https://doi.org/10.1016/j.marenvres.2013.05.005.
3) Brakstad O.G., Ribicic D., Winkler A., Netzer R. (2018). Biodegradation of dispersed oil in seawater is not inhibited by a commercial oil spill dispersant. Mar. Pollut. Bull. 129 555–561. https://doi.org/10.1016/j.marpolbul.2017.10.030.
4) Brakstad O.G., Throne-Holst M., Netzer R., Stoeckel D.M., Atlas R.M. (2015). Microbial communities related to biodegradation of dispersed Macondo oil at low seawater temperature with Norwegian coastal seawater. Microb. Biotechnol. 8 989–998. https://doi.org/10.1111/1751-7915.12303.

5) Callahan B.J., McMurdie P.J., Rosen M.J., Han A.W., Johnson A.J.A., Holmes S.P. (2016). DADA2: High-resolution sample inference from Illumina amplicon data. Nat. Methods. 13 581–583. https://doi.org/10.1038/nmeth.3869.

6) Frette L., Winding A., Kroer N. (2010). Genetic and metabolic diversity of arctic bacterioplankton during the post-spring phytoplankton bloom in Disko Bay, western Greenland. Aquat. Microb. Ecol. 60 29–41. https://doi.org/10.3354/ame01410.

7) Gallotta F.D.C., Christensen J.H. (2012). Source identification of petroleum hydrocarbons in soil and sediments from Iguaçu River Watershed, Paraná, Brazil using the CHEMSIC method (CHEMometric analysis of Selected Ion Chromatograms). J. Chromatogr. A. 1235 149–158. https://doi.org/10.1016/j.chroma.2012.02.041.

8) Geng X., Boufadel M.C., Personna Y.R., Lee K., Tsao D., Demicco E.D. (2014). BIOB: A mathematical model for the biodegradation of low solubility hydrocarbons. Mar. Pollut. Bull. 83 138–147. https://doi.org/10.1016/j.marpolbul.2014.04.007.

9) Gluchowska M., Trudnowska E., Goszczko I., Kubiszyn A.M., Blachowiak-Samolyk K., Walczowski W., Kwasniewski S. (2017). Variations in the structural and functional diversity of zooplankton over vertical and horizontal environmental gradients en route to the Arctic Ocean through the Fram Strait. PLoS One. 12 1–26. https://doi.org/10.1371/journal.pone.0171715.

10) Gomes A., Christensen J.H., Gründger F., Kjeldsen K.U., Rysgaard S., Vergeynst L. (2022). Biodegradation of water-accommodated aromatic oil compounds in Arctic seawater at 0 °C, Chemosphere. 286 (2022). https://doi.org/10.1016/j.chemosphere.2021.131751.

11) Guo R., Liang Y., Xin Y., Wang L., Mou S., Cao C., Xie R., Zhang C., Tian J., Zhang Y. (2018). Insight Into the Pico- and Nano-Phytoplankton Communities in the Deepest Biosphere, the Mariana Trench, Front. Microbiol. 9 1–14. https://doi.org/10.3389/fmicb.2018.02289.

12) Hauptfeld E., Pelkmans J., Huisman T.T., Anocic A., Snoek B.L., von Meijenfeldt F.A.B., Gerritse J., van Leeuwen J., Leurink G., van Lit A., van Uffelen R., Koster M.C., Dutilh B.E. (2022). A metagenomic portrait of the microbial community responsible for two decades of bioremediation of poly-contaminated groundwater, Water Res. 221 118767. https://doi.org/10.1016/j.watres.2022.118767.

13) Head I.M., Jones D.M., Röling W.F.M. (2006). Marine microorganisms make a meal of oil. Nat. Rev. Microbiol. 4 173–182. https://doi.org/10.1038/nrmicro1348.

14) Herlemann D.P.R., Labrenz M., Jürgens K., Bertilsson S., Waniek J.J., Andersson A.F. (2011). Transitions in bacterial communities along the 2000 km salinity gradient of the Baltic Sea, ISME J. 5 1571–1579. https://doi.org/10.1038/ismej.2011.41.

15) Horel A., Mortazavi B., Sobecky P.A. (2012). Responses of microbial community from northern Gulf of Mexico sandy sediments following exposure to deepwater horizon crude oil. Environ. Toxicol. Chem. 311004–1011. https://doi.org/10.1002/etc.1770.

16) Kay M., Elkin L., Higgins J., Wobbrock J. (2021). ARTool: Aligned Rank Transform for Nonparametric Factorial ANOVAs. R package version 0.11.1, https://github.com/mjskay/ARTool.

17) Kimes N.E., Callaghan A. V., Suflita J.M., Morris P.J. (2014). Microbial transformation of the deepwater horizon oil spill-past, present, and future perspectives. Front. Microbiol. 5 (2014) 1–11. https://doi.org/10.3389/fmicb.2014.00603.

18) Kristensen M., Johnsen A.R., Christensen J.H. (2015). Marine biodegradation of crude oil in temperate and Arctic water samples. J. Hazard. Mater. 300 75–83. https://doi.org/10.1016/j.jhazmat.2015.06.046.

19) Li M., Garrett C. (1998). The relationship between oil droplet size and upper ocean turbulence. Mar. Pollut. Bull. 36 961–970. https://doi.org/10.1016/S0025-326X(98)00096-4.

20) Lofthus S., Bakke I., Greer C.W., Brakstad O.G. (2021). Biodegradation of weathered crude oil by microbial communities in solid and melted sea ice. Mar. Pollut. Bull. 172. https://doi.org/10.1016/j.marpolbul.2021.112823

21) Lozupone C., Lladser M.E., Knights D., Stombaugh J., Knight R. (2011). UniFrac: An effective distance metric for microbial community comparison. ISME J. 5 169–172. https://doi.org/10.1038/ismej.2010.133.

22) Lever M.A., Torti A., Eickenbusch P., Michaud A.B., Šantl-Temkiv T., Jørgensen B.B. (2015). A modular method for the extraction of DNA and RNA, and the separation of DNA pools from diverse environmental sample types, Front. Microbiol. 6 https://doi.org/10.3389/fmicb.2015.00476.

23) Margesin R., Schinner F. (1999). Biological decontamination of oil spills in cold environments. J. Chem. Technol. Biotechnol. 74 381–389. https://doi.org/10.1002/(SICI)1097-4660(199905)74:5<381::AID-JCTB59>3.0.CO;2-0.

24) Meire L., Mortensen J., Rysgaard S., Bendtsen J., Boone W., Meire P., Meysman F.J.R. (2016) Spring bloom dynamics in a subarctic fjord influenced by tidewater outlet glaciers (Godthåbsfjord, SW Greenland). J. Geophys. Res. Biogeosciences. 121 1581–1592. https://doi.org/10.1002/2015JG003240.

25) Middelboe M., Glud R.N., Sejr M.K. (2012). Bacterial carbon cycling in a subarctic fjord: A seasonal study on microbial activity, growth efficiency, and virus-induced mortality in Kobbefjord, Greenland, Limnol. Oceanogr. 57 1732–1742. https://doi.org/10.4319/lo.2012.57.6.1732.

26) Miller, A.W., Ruiz, G.M. (2014). Arctic shipping and marine invaders. Nat. Clim. Chang. 4, 413–416. https://doi.org/10.1038/nclimate2244

27) Mortensen J., Lennert K., Bendtsen J., Rysgaard S. (2011). Heat sources for glacial melt in a sub-Arctic fjord (Godthåbsfjord) in contact with the Greenland Ice Sheet. J. Geophys. Res. Ocean. 116 1–13. https://doi.org/10.1029/2010JC006528.

28) Murphy S.M.C., Bautista M.A., Cramm M.A., Hubert C.R.J. (2021). Diesel and Crude Oil Biodegradation by Cold-Adapted Microbial Communities in the Labrador Sea. Appl. Environ. Microbiol. 87 1–21. https://doi.org/10.1128/AEM.00800-21.

29) Nikolova C., Gutierrez T. (2022). Marine hydrocarbon-degrading bacteria: their role and application in oil-spill response and enhanced oil recovery. INC. https://doi.org/10.1016/b978-0-323-85455-9.00005-9.

30) Nõlvak H., Dang N.P., Truu M., Peeb A., Tiirik K., O'sadnick M., Truu J. (2021). Microbial community dynamics during biodegradation of crude oil and its response to biostimulation in svalbard seawater at low temperature. Microorganisms. 9 1–23. https://doi.org/10.3390/microorganisms9122425.

31) Oksanen J., Blanchet F.G., Friendly M., Kindt R., Legendre P., McGlinn D., Minchin P.R., O'Hara R.B., Simpson G.L., Solymos P.M., Stevens H.H., Szoecs E., Wagner H. (2019). vegan R package: an R package for community ecologists. R package version 2.5-6. https://cran.rproject.org/package=vegan

32) Omarova M., Swientoniewski L.T., Mkam Tsengam I.K., Blake D.A., John V., McCormick A., Bothun G.D., Raghavan S.R., Bose A. (2019). Biofilm Formation by Hydrocarbon-Degrading Marine Bacteria and Its Effects on Oil Dispersion, ACS Sustain. Chem. Eng. 7 14490–14499. https://doi.org/10.1021/acssuschemeng.9b01923.

33) Péquin B., Cai Q., Lee K., Greer C.W. (2022). Natural attenuation of oil in marine environments: A review. Mar. Pollut. Bull. 176 https://doi.org/10.1016/j.marpolbul.2022.113464.

34) Potts L.D., Perez Calderon L.J., Gontikaki E., Keith L., Gubry-Rangin C., Anderson J.A., Witte U. (2018). Effect of spatial origin and hydrocarbon composition on bacterial consortia community structure and hydrocarbon biodegradation rates. FEMS Microbiol. Ecol. 94 1–12. https://doi.org/10.1093/femsec/fiy127.

35) Potts L.D., Perez Calderon L.J., Gontikaki E., Keith L., Gubry-Rangin C., Anderson J.A., Witte U. (2018). Effect of spatial origin and hydrocarbon composition on bacterial consortia community structure and hydrocarbon biodegradation rates. FEMS Microbiol. Ecol. 94 1–12. https://doi.org/10.1093/femsec/fiy127.

36) Powell S.M., Harvey P.M.A., Stark J.S., Snape I., Riddle M.J. (2007). Biodegradation of petroleum products in experimental plots in Antarctic marine sediments is location dependent, Mar. Pollut. Bull. 54 (2007) 434–440. https://doi.org/10.1016/j.marpolbul.2006.11.018.

37) Price M.N., Dehal P.S., Arkin A.P. (2010). FastTree 2 - Approximately maximum-likelihood trees for large alignments. PLoS One. 5. https://doi.org/10.1371/journal.pone.0009490.

38) Quast C., Pruesse E., Yilmaz P., Gerken J., Schweer T., Yarza P., Peplies J., Glöckner F.O. (2013). The SILVA ribosomal RNA gene database project: Improved data processing and web-based tools. Nucleic Acids Res. 41 590–596. https://doi.org/10.1093/nar/gks1219.

39) R Core Team, 2019. R: a language and environment for statistical computing; R Foundation for Statistical Computing; Vienna; Austria. http://www.r-project.org/index.html.

40) Randelhoff A., Lacour L., Marec C., Leymarie E., Lagunas J., Xing X., Darnis G.,. Penkerc C, Sampei M., Fortier L.,. D'Ortenzio F, Claustre H., Babin M. (2020). Arctic mid-winter phytoplankton growth revealed by autonomous profilers. Sci. Adv. 6 1–10. https://doi.org/10.1126/sciadv.abc2678.

638 41) Reigstad M., Wassmann P., Wexels Riser C., Øygarden S., Rey F. (2002). Variations in
639 hydrography, nutrients and chlorophyll a in the marginal ice-zone and the central Barents Sea. J.
640 Mar. Syst. 38 9–29. https://doi.org/10.1016/S0924-7963(02)00167-7.

641 42) Ribicic D., McFarlin K.M., Netzer R., Brakstad O.G., Winkler A., Throne-Holst M., Størseth T.R.
642 (2018). Oil type and temperature dependent biodegradation dynamics - Combining chemical and
643 microbial community data through multivariate analysis. BMC Microbiol. 18 (2018) 1–15.
644 https://doi.org/10.1186/s12866-018-1221-9.

645 43) Ron E.Z., Rosenberg E. (2014). Enhanced bioremediation of oil spills in the sea. Curr. Opin.
646 Biotechnol. 27 191–194. https://doi.org/10.1016/j.copbio.2014.02.004.

647 44) Sala M.M., Arrieta J.M., Boras J.A., Duarte C.M., Vaqué D. (2010). The impact of ice melting
648 on bacterioplankton in the Arctic Ocean. Polar Biol. 33 1683–1694.
649 https://doi.org/10.1007/s00300-010-0808-x.

650 45) Scheibye K., Christensen J.H., Johnsen A.R. (2017). Biodegradation of crude oil in Arctic
651 subsurface water from the Disko Bay (Greenland) is limited. Environ. Pollut. 223 73–80.
652 https://doi.org/10.1016/j.envpol.2016.12.032.

653 46) Schweitzer H.D., Smith H.J., Barnhart E.P., McKay L.J., Gerlach R., Cunningham A.B.,
654 Malmstrom R.R., Goudeau D., Fields M.W. (2022). Subsurface hydrocarbon degradation
655 strategies in low- and high-sulfate coal seam communities identified with activity-based
656 metagenomics. Npj Biofilms Microbiomes. 8 https://doi.org/10.1038/s41522-022-00267-2.

657 47) Sejr M.K., Krause-Jensen D., Dalsgaard T., Ruiz-Halpern S., Duarte C.M., Middelboe M., Glud
658 R.N., Bendtsen J., Balsby T.J.S., Rysgaard S. (2014). Seasonal dynamics of autotrophic and
659 heterotrophic plankton metabolism and PCO2 in a subarctic Greenland fjord. Limnol. Oceanogr.
660 59 1764–1778. https://doi.org/10.4319/lo.2014.59.5.1764.

48) Shankar R., Shim W.J., An J.G., Yim U.H. (2015). A practical review on photooxidation of crude oil: Laboratory lamp setup and factors affecting it, Water Res. 68 304–315. https://doi.org/10.1016/j.watres.2014.10.012.

49) Shiller A.M., Joung D. (2012). Nutrient depletion as a proxy for microbial growth in Deepwater Horizon subsurface oil/gas plumes. Environ. Res. Lett. 7 https://doi.org/10.1088/1748-9326/7/4/045301.

50) Singh A.K., Sherry A., Gray N.D., Jones D.M., Bowler B.F.J., Head I.M. (2012). Kinetic parameters for nutrient enhanced crude oil biodegradation in intertidal marine sediments. Front. Microbiol. 5 (2014) 1–13. https://doi.org/10.3389/fmicb.2014.00160.

51) Skov T., Van Den Berg F., Tomasi G., Bro R. (2006). Automated alignment of chromatographic data. J. Chemom. 20 484–497. https://doi.org/10.1002/cem.1031.

52) Starnawski P., Bataillon T., Ettema T.J.G., Jochum L.M., Schreiber L., Chen X., Lever M.A., Polz M.F., Jørgensen B.B., Schramm A., Kjeldsen K.U. (2017). Microbial community assembly and evolution in subseafloor sediment. Proc. Natl. Acad. Sci. U. S. A. 114 2940–2945. https://doi.org/10.1073/pnas.1614190114.

53) Tamelander T., Kivimäe C., Bellerby R.G.J., Renaud P.E., Kristiansen S. (2009). Base-line variations in stable isotope values in an Arctic marine ecosystem: Effects of carbon and nitrogen uptake by phytoplankton. Hydrobiologia. 630 63–73. https://doi.org/10.1007/s10750-009-9780-2.

54) Teramoto M., Suzuki M., Hatmanti A., Harayama S. 2010. The potential of Cycloclasticus and Altererythrobacter strains for use in bioremediation of petroleum-aromatic-contaminated tropical marine environments. J. Biosci. Bioeng. 110 48–52. https://doi.org/10.1016/j.jbiosc.2009.12.008.

55) Tissot, B.P., Welte, D.H. (1978). Petroleum Formation and Occurrence, Petroleum Formation and Occurrence. https://doi.org/10.1007/978-3-642-96446-6

56) Tomasi G., Savorani F., Engelsen S.B. (2011). Icoshift: An effective tool for the alignment of chromatographic data, J. Chromatogr. A. 1218 7832–7840. https://doi.org/10.1016/j.chroma.2011.08.086.

57) Tomasi G., Van Den Berg F., Andersson C. (2004). Correlation optimized warping and dynamic time warping as preprocessing methods for chromatographic data. J. Chemom. 18 231–241. https://doi.org/10.1002/cem.859.

58) Tremblay J.É., Robert D., Varela D.E., Lovejoy C., Darnis G., Nelson R.J., Sastri A.R. (2012). Current state and trends in Canadian Arctic marine ecosystems: I. Primary production. Clim. Change. 115 161–178. https://doi.org/10.1007/s10584-012-0496-3.

59) Vergeynst L., Christensen J.H., Kjeldsen K.U., Meire L., Boone W., Malmquist L.M.V., Rysgaard S. (2019a). In situ biodegradation, photooxidation and dissolution of petroleum compounds in Arctic seawater and sea ice. (2019a). Wat. Res. Water Research, 148, 1, 459-468 https://doi.org/10.1016/j.watres.2018.10.066.

60) Vergeynst L., Greer C.W., Mosbech A., Gustavson K., Meire L., Poulsen K.G., Christensen J.H. (2019b). Biodegradation, Photo-oxidation, and Dissolution of Petroleum Compounds in an Arctic Fjord during Summer, Environ. Sci. Technol. 53 12197–12206. https://doi.org/10.1021/acs.est.9b03336.

61) Vergeynst L., Kjeldsen K.U., Lassen P., Rysgaard S. (2018b). Bacterial community succession and degradation patterns of hydrocarbons in seawater at low temperature. J. Hazard. Mater. 353 127–134. https://doi.org/10.1016/j.jhazmat.2018.03.051.

62) Vergeynst L., Wegeberg S., Aamand J., Lassen P., Gosewinkel U., Fritt-Rasmussen J., Gustavson K., Mosbech A. (2018a). Biodegradation of marine oil spills in the Arctic with a Greenland perspective. Sci. Total Environ. 626 1243–1258. https://doi.org/10.1016/j.scitotenv.2018.01.173.

63) Wang Q., Garrity G.M., Tiedje J.M., Cole J.R. (2017). Naïve Bayesian classifier for rapid assignment of rRNA sequences into the new bacterial taxonomy. Appl. Environ. Microbiol. 73 5261–5267. https://doi.org/10.1128/AEM.00062-07.

64) Wickham H. (2016). ggplot2: Elegant Graphics for Data Analysis; Springer

65) Wickham H., Averick M., Bryan J., Chang W., McGowan L., François R., Grolemund G., Hayes A., Henry L., Hester J., Kuhn M., Pedersen T., Miller E., Bache S., Müller K., Ooms J., Robinson D., Seidel D., Spinu V., Takahashi K., Vaughan D., Wilke C., Woo K., Yutani H. (2019). Welcome to the Tidyverse, J. Open Source Softw. 4 1686. https://doi.org/10.21105/joss.01686.

66) Xue J., Yu Y., Bai Y., Wang L., Wu Y. (2015). Marine Oil-Degrading Microorganisms and Biodegradation Process of Petroleum Hydrocarbon in Marine Environments: A Review. Curr. Microbiol. 71 220–228. https://doi.org/10.1007/s00284-015-0825-7.

67) Yilmaz P., Parfrey L.W., Yarza P., Gerken J., Pruesse E., Quast C., Schweer T., Peplies J., Ludwig W., Glöckner F.O. (2014). The SILVA and "all-species Living Tree Project (LTP)" taxonomic frameworks, Nucleic Acids Res. 42 643–648. https://doi.org/10.1093/nar/gkt1209.

68) Brakstad, O.G., Bonaunet, K., 2006. Biodegradation of petroleum hydrocarbons in seawater at low temperatures (0-5°C) and bacterial communities associated with degradation. Biodegradation 17, 71–82. https://doi.org/10.1007/s10532-005-3342-8

69) McFarlin, K.M., Prince, R.C., Perkins, R., Leigh, M.B., 2014. Biodegradation of dispersed oil in Arctic seawater at -1°C. PLoS One 9, 1–8. https://doi.org/10.1371/journal.pone.0084297

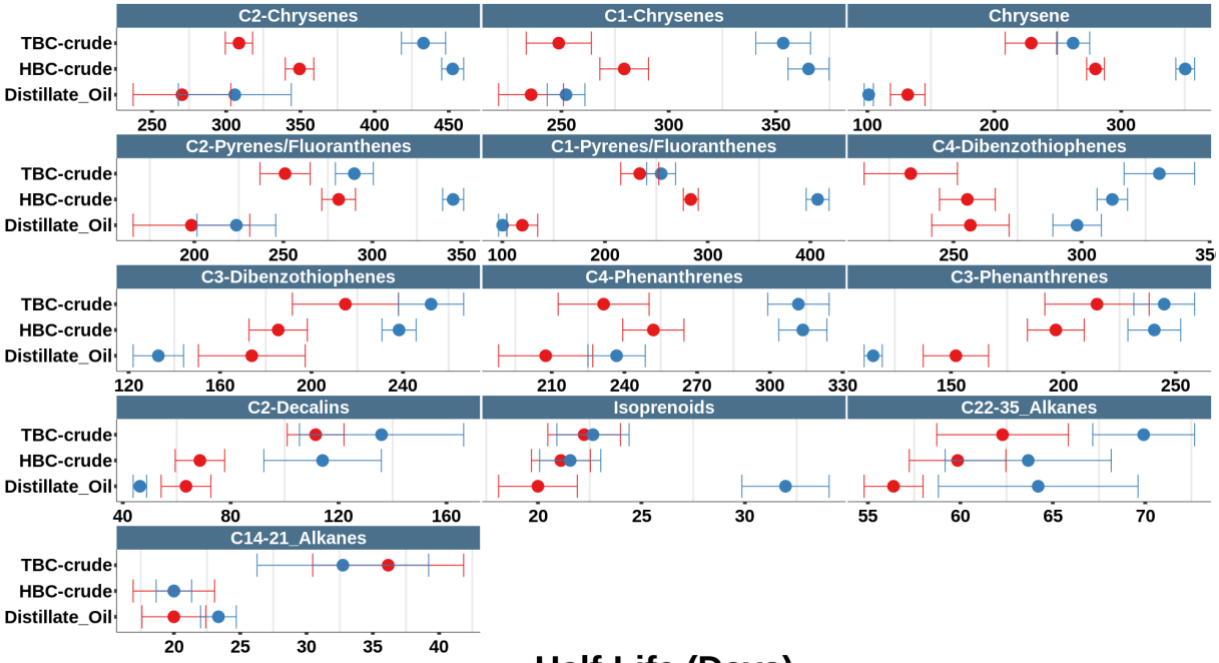

Figure 1. Estimated half-life times with standard error of three types of oil in the mesopelagic (red) and epipelagic zone (blue). TBC: troll blend crude oil, HBC: high in-source biodegraded crude oil

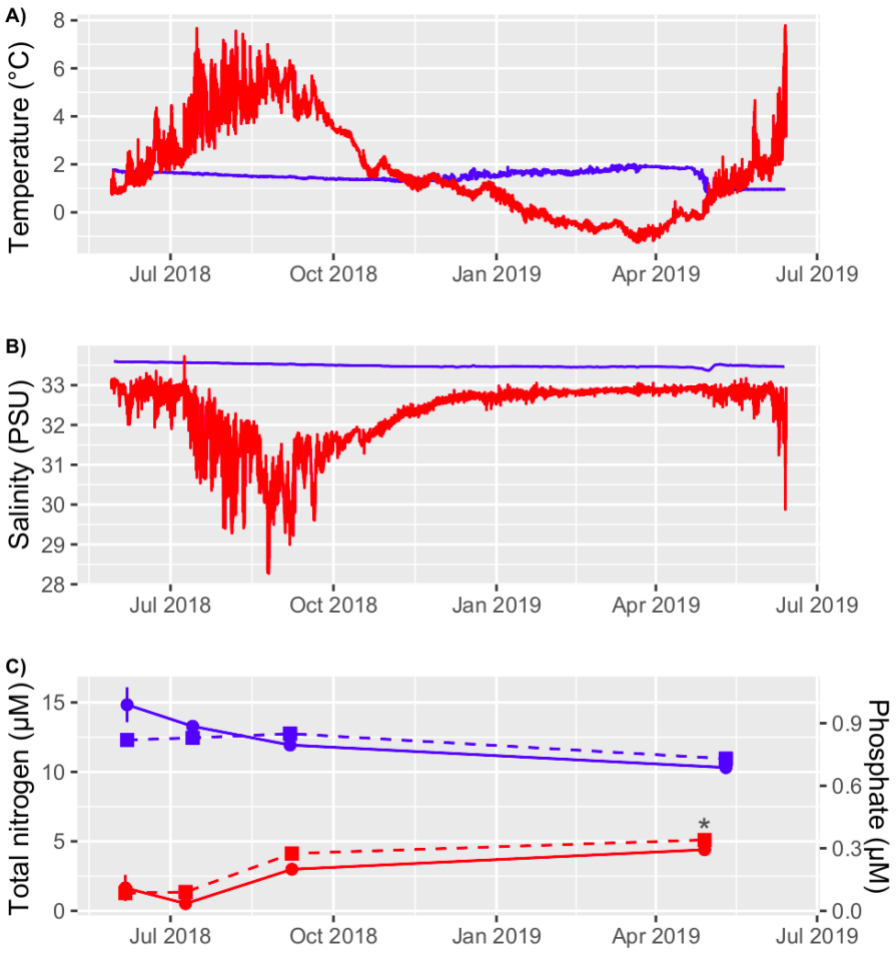

Figure 2. Temperature (A), salinity (B) and total-nitrogen/phosphorus data (C) measured in the mesopelagic (blue) and epipelagic zone (red) over the course of one year during the experimental period. *Data sample for the nutrients in Kobbefjord (epipelagic zone) was taken in April 2016 and not April 2019. The point was added for showing the typical seasonal variation of the nutrient concentrations in the epipelagic zone, as also previously observed (Sejr et al., 2014).

741

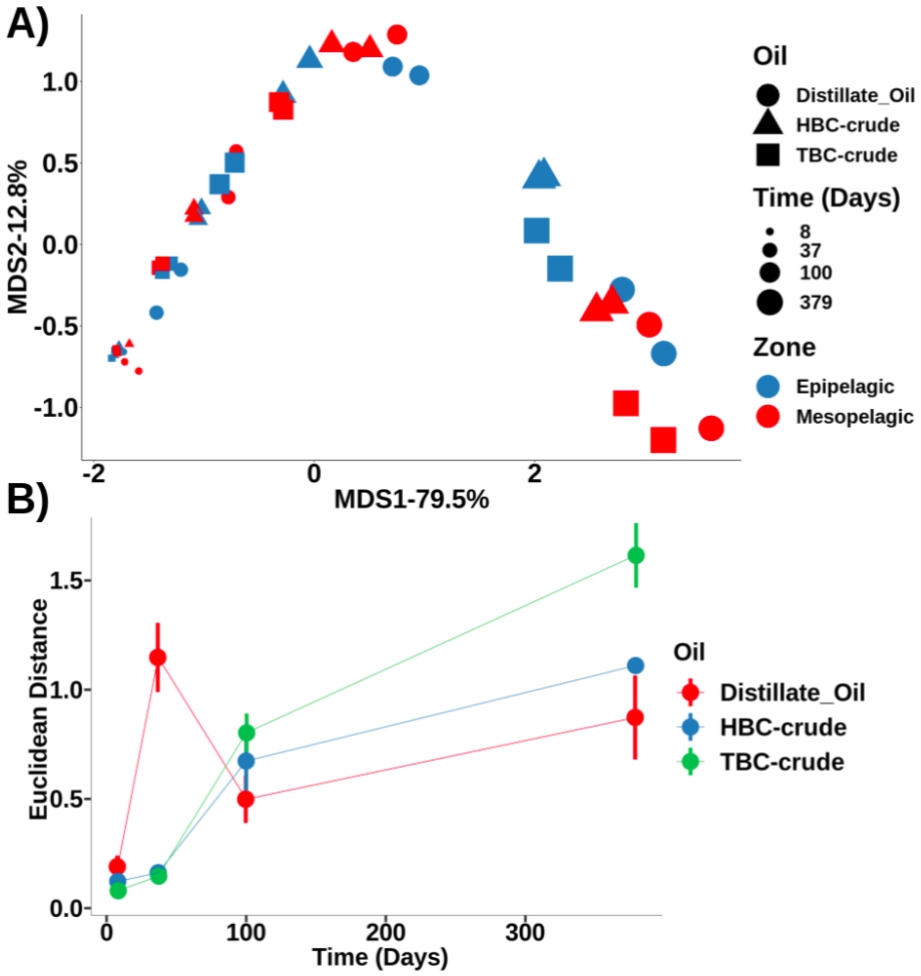

742

743 **Figure 3.** A) Multi-dimensional scaling ordination plot that visualizes the changes in hydrocarbon
744 composition (Euclidean distance). B) Difference of hydrocarbon composition (Euclidean distance)
745 between the two zones over time (n=2). TBC: troll blend crude oil, HBC: high in-source biodegraded
746 crude oil.

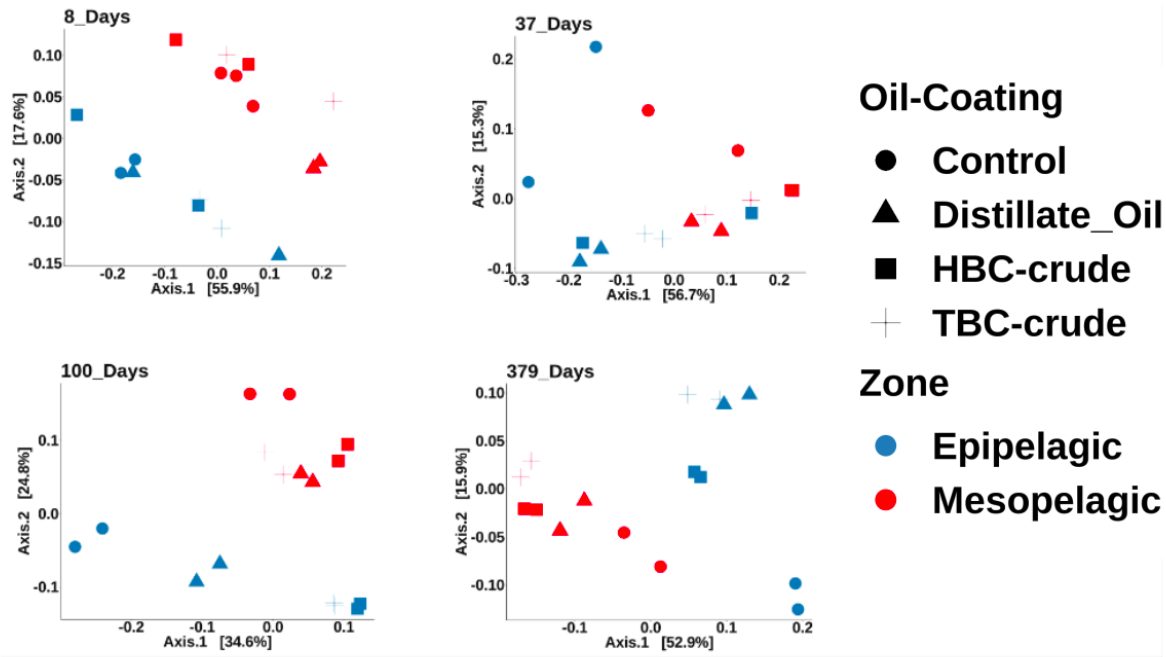

Figure 4. Multi-dimensional scaling (MDS) plots based on weighed Unifrac distances showing the β-diversity profile of oil-coated and non-coated samples. We separated the four time points to visualize the influence of oil-exposure and zone on bacterial communities: day 8, 37, 100 and 379. The graphs visualize how both zone and oil exposure contributed to the differences in community composition as a function of time. TBC: troll blend crude oil, HBC: high in-source biodegraded crude oil.

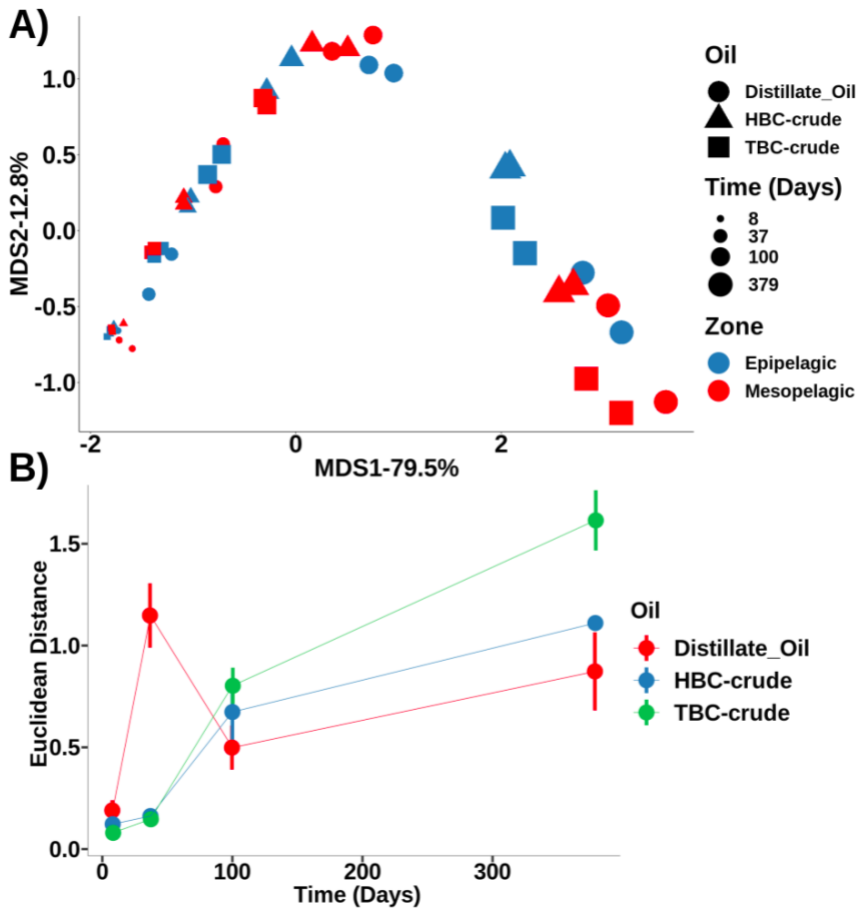

Figure 5. A) Regression plot of dissimilarities of bacterial community composition based on weighed Unifrac distance versus dissimilarities of hydrocarbon composition based on Euclidean distance (576 sample dissimilarities). The correlation of β-diversity and hydrocarbon composition was verified by a Mantel test (r = 0.68, p = 1x10^{-5}, n=24). B) Procrustes plot showing the association between the bacterial community and hydrocarbon composition. Procrustes rotation was used to rotate the dissimilarity matrix of the bacterial community composition (β-diversity, Weighted Unifrac Distance) to maximum similarity with the target dissimilarity matrix of the hydrocarbon composition (Euclidean distance) by minimizing the sum of squared differences. The Procrustes plot visualizes the association between bacterial community and poor water-soluble hydrocarbon composition (Procrustes correlation r = 0.8, p = 1 x 10^{-5}). The length of the arrows visualizes the degree of match between the two ordinations following Procrustes rotation (arrow-start: β-diversity, arrow-end: Hydrocarbon composition). TBC: troll blend crude oil, HBC: high in-source biodegraded crude oil.

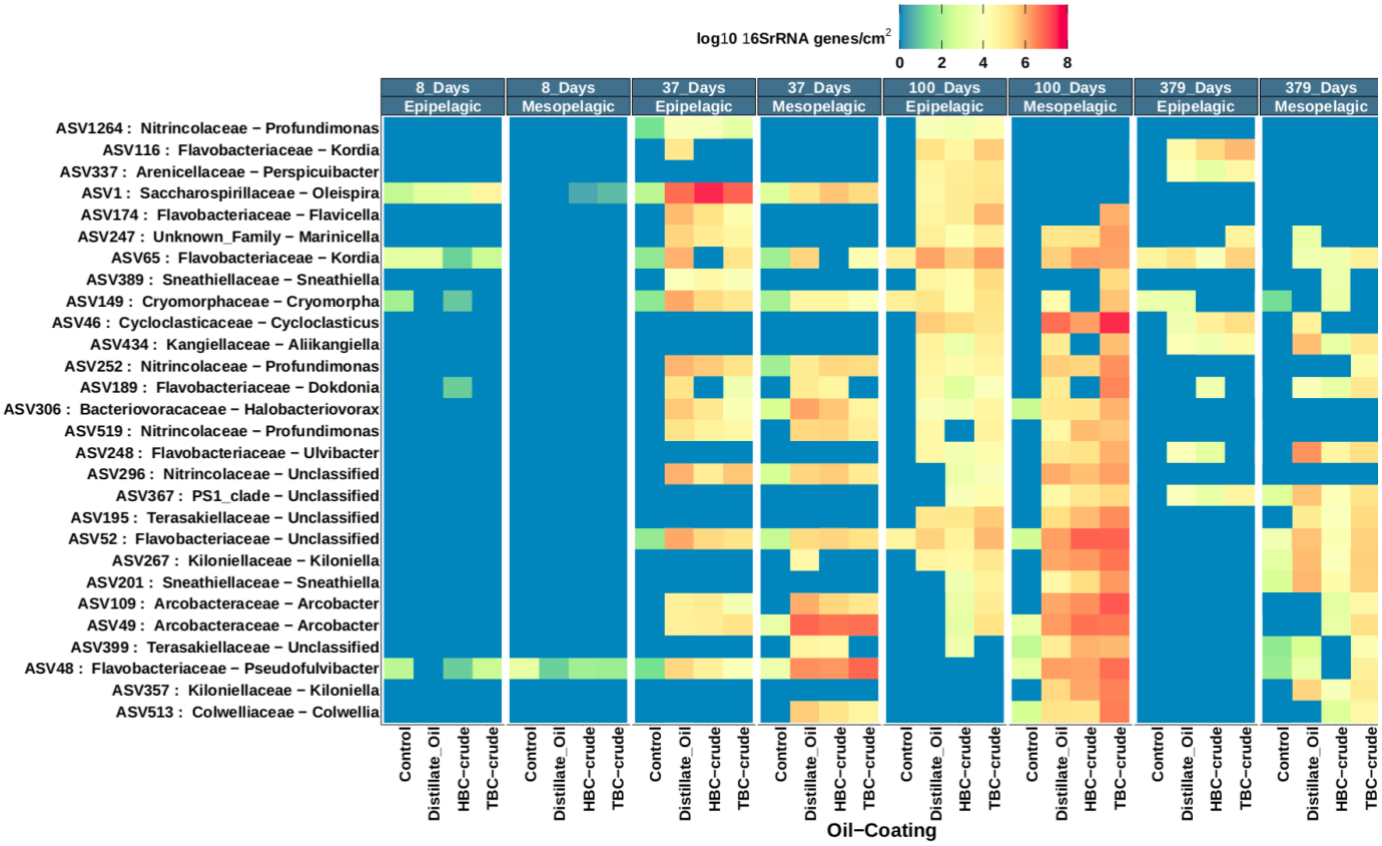

Figure 6. Densities (qPCR quantification determined via qPCR x Relative abundance determined by amplicon sequencing) of oil-associated ASVs that significantly differed between the oil-coated and non-coated samples (average of duplicates). ASVs on the y-axis were ordered by increasing difference between the densities in the epipelagic versus mesopelagic zone. The black line separates the ASVs with higher densities in epipelagic zone (upper part) and the ASV with higher densities in mesopelagic zone (lower part). The plot depicts only oil-associated ASVs with *p*-value lower than 0.001 (Aligned-Rank Transform ANOVA and Benjamini-Hochberg correction). The full list of oil-associated ASVs is provided in Table S3. TBC: troll blend crude oil, HBC: high in-source biodegraded crude oil.

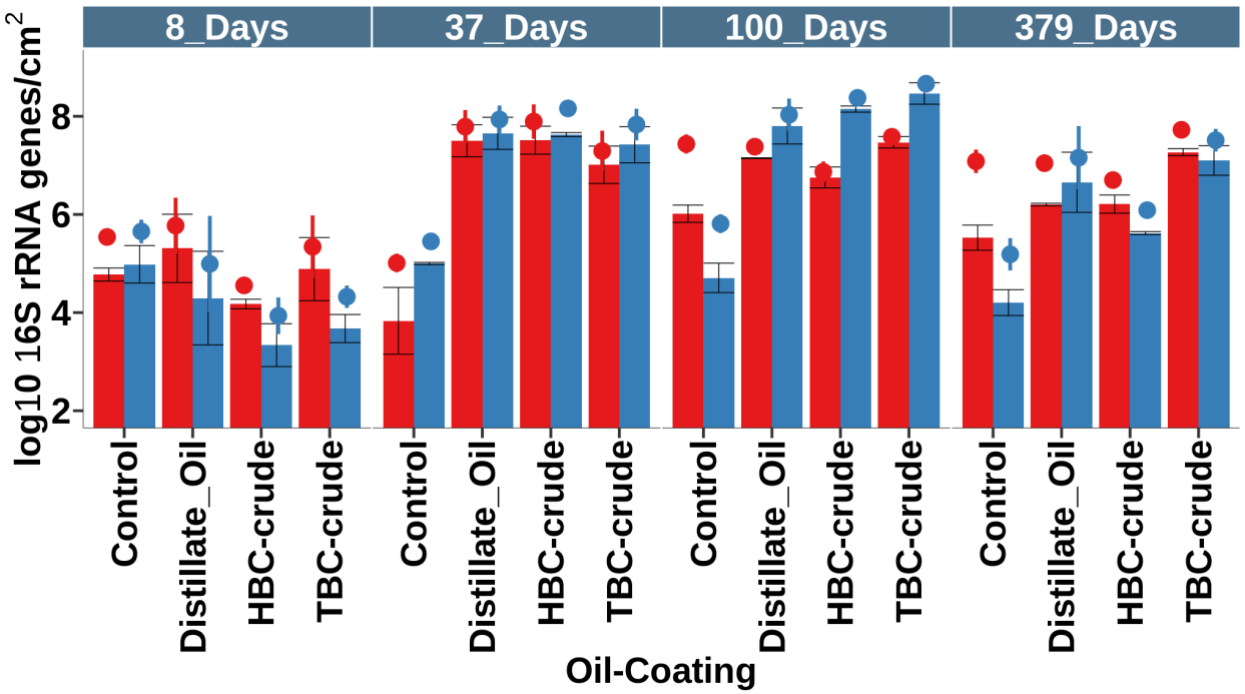

Figure 7. Cumulative density (sum of densities) of oil associated ASVs (barplot) and total-bacterial densities (dotplot) in oil-coated adsorbents (average of duplicates), for epipelagic (blue) and mesopelagic (red) adsorbents. Densities were calculated by multiplying the number of 16S rRNA genes determined by qPCR with the relative gene abundances determined by amplicon sequencing. TBC: troll blend crude oil, HBC: high in-source biodegraded crude oil.

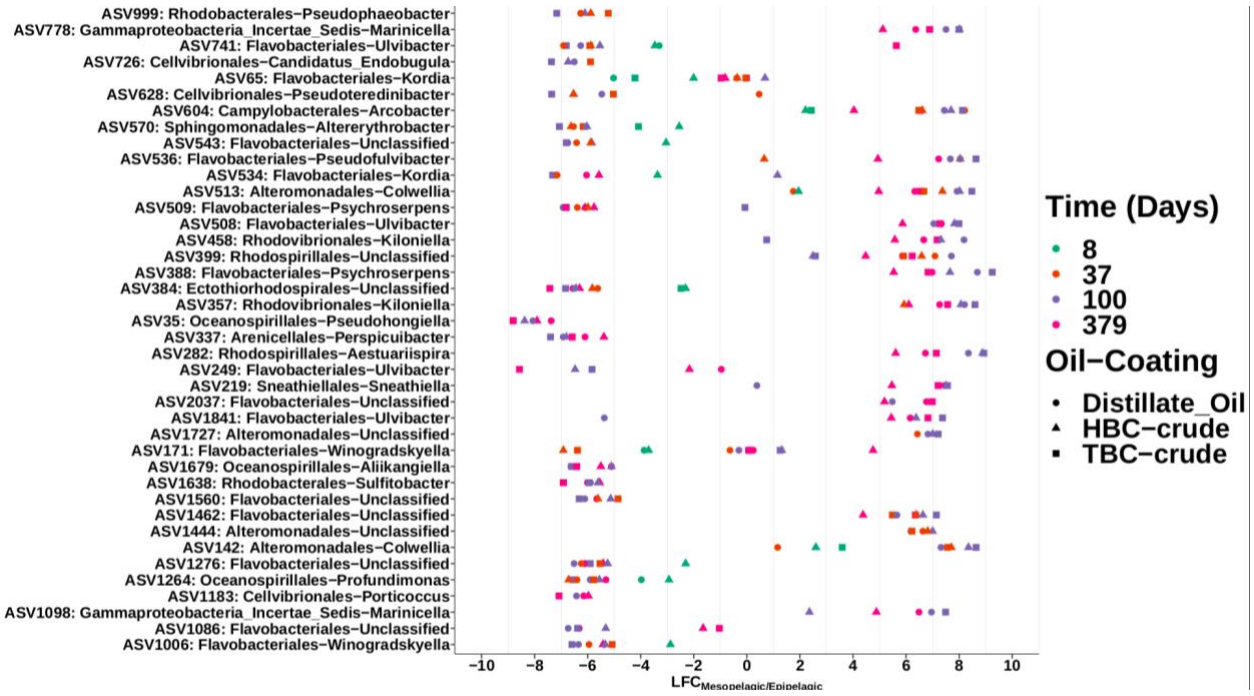

Figure 8. Log_{10} fold change (LFC) of densities (16S rRNA genes/cm^2) between the two zones for oil-associated ASVs for which the density differed significantly between the zones ($p < 0.05$ Aligned-Rank Transform ANOVA and Benjamini-Hochberg correction). TBC: troll blend crude oil, HBC: high in-source biodegraded crude oil.